COMPRESSED SENSING FOR WIDEBAND COGNITIVE RADIOS

Zhi Tian

Dept. of Electrical & Computer Engineering
Michigan Technological University
Houghton, MI 49931 USA

Georgios B. Giannakis

Dept. of Electrical & Computer Engineering
University of Minnesota
Minneapolis, MN 55455 USA

ABSTRACT

In the emerging paradigm of open spectrum access, cognitive radios dynamically sense the radio-spectrum environment and must rapidly tune their transmitter parameters to efficiently utilize the available spectrum. The unprecedented radio agility envisioned, calls for fast and accurate spectrum sensing over a wide bandwidth, which challenges traditional spectral estimation methods typically operating at or above Nyquist rates. Capitalizing on the sparseness of the signal spectrum in open-access networks, this paper develops compressed sensing techniques tailored for the coarse sensing task of spectrum hole identification. Sub-Nyquist rate samples are utilized to detect and classify frequency bands via a wavelet-based edge detector. Because spectrum location estimation takes priority over fine-scale signal reconstruction, the proposed novel sensing algorithms are robust to noise and can afford reduced sampling rates.

Index Terms— spectrum estimation, compressed sensing, sub-Nyquist sampling, wavelet transform, cognitive radio

1. INTRODUCTION

The emerging paradigm of Dynamic Spectrum Access shows promise to alleviate today's spectrum scarcity problem by ushering in new forms of spectrum agile wireless networks [1]. Key to this new paradigm are cognitive radios (CRs) that are aware of and can sense the environments, and perform functions to best serve their users without causing harmful interference to other authorized users [2]. As such, the first cognitive task preceding any form of dynamic spectrum management is to develop wireless spectral detection and estimation techniques for sensing and identification of available spectrum.

Spectrum sensing in the wideband regime faces considerable technical challenges. The radio front-end can employ a bank of tunable narrowband bandpass filters to search one narrow frequency band at a time. In each narrowband, existing spectrum sensing techniques perform either energy detection [3] or feature detection [2]. It requires an unfavorably large number of RF components and the tuning range of each filter is preset. Alternatively, a wideband circuit utilizes a single RF chain followed by high-speed DSP to flexibly search over multiple frequency bands concurrently [4]. A major implementation challenge lies in the very high sampling rates required by conventional spectral estimation methods which have to operate at or above the Nyquist rate. Meanwhile, due to the timing requirements for rapid sensing, only a limited number of measurements can be acquired from the received signal, which may not provide sufficient statistic when traditional linear signal reconstruction methods are employed.

This paper aims at fast spectrum sensing at affordable complexity. A couple of key premises are capitalized to alleviate the stringent sampling requirements in the wideband regime. First, we take a multi-resolution approach to decompose the cognitive sensing task into two stages. The first stage is coarse sensing to detect non-overlapping spectrum bands and classify them into *black, gray* or *white* spaces, depending on whether the power spectral density (PSD) levels are high, medium or low [2]. Based on the spectrum sharing mechanism adopted [1], the second stage of fine-scale spectral shape estimation is performed only when needed, and mostly confined within the available (narrowband) white spaces to alleviate the sampling requirements. Second, we recognize that the wireless signals in open-spectrum networks are typically *sparse* in the frequency domain. This is due to the low percentage of spectrum occupancy by active radios – a fact motivating dynamic spectrum management. For sparse signals, recent advances in compressed sensing have demonstrated the principle of sub-Nyquist-rate sampling and reliable signal recovery via computationally feasible algorithms [5, 6, 7, 8].

Tailored to the above distinct nature of CR sensing, this paper derives novel compressed sensing algorithms for the coarse sensing task of spectrum band classification. Random sub-Nyquist-rate samples are employed to formulate an optimal signal reconstruction problem, which incorporates the wavelet-based edge detector we recently developed in [10] to recover the locations of frequency bands. Because spectrum location estimation takes priority over fine-scale signal reconstruction, the novel sensing algorithms are robust to noise and can afford reduced sampling rates.

2. SIGNAL MODEL AND PROBLEM STATEMENT

Suppose that a total of B Hz in the frequency range $[f_0, f_N]$ is available for a wideband wireless network. A CR receives the signal $r(t)$ that occupies N consecutive spectrum bands, with their frequency boundaries located at $f_0 < f_1 < \cdots f_N$. The frequency response of $r(t)$ is illustrated in Fig. 1. Depending on whether the PSD level is high, medium or low, each frequency segment can be categorized into black, gray or white spectrum spaces [2]. White holes, and sometimes gray spaces, can be picked by the CR for opportunistic transmission, while the black holes are to be avoided for interference control.

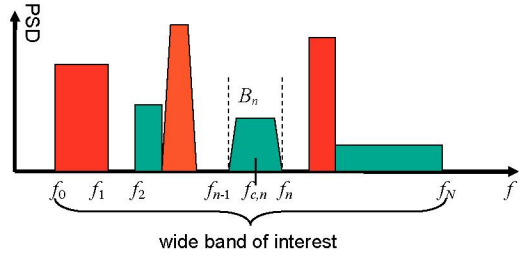

Fig. 1. N frequency bands with piecewise smooth PSD.

Suppose that the time window for sensing is $t \in [0, MT_0]$, where T_0 is the Nyquist sampling rate. Using Nyquist sampling theory, M samples are needed to recover $r(t)$ without aliasing. A digital receiver converts the continuous-domain signal $r(t)$ to a discrete sequence $\mathbf{x}_t \in \mathcal{C}^K$ of length K. The sampling process can be expressed in discrete-time domain in the following general form:

$$\mathbf{x}_t = \mathbf{S}^T \mathbf{r}_t \tag{1}$$

where $\mathbf{S}$ is an $M \times K$ projection matrix and $\mathbf{r}_t$ represents the $M \times 1$ vector with elements $r_t[n] = r(t)|_{t=nT_0}$, $n = 1, \ldots, M$. Columns $\{\mathbf{s}_k\}_{k=1}^K$ of $\mathbf{S}$ can be viewed as a set of basis signals or matched filters, while the measurements $\{x_t[k]\}_{k=1}^K$ are in essence the projection of $r(t)$ onto the basis. The model in (1) subsumes all sampling schemes yielding linear measurements. For example, $\mathbf{S} = \mathbf{I}_M$ represents Nyquist-rate uniform sampling, where $\mathbf{I}_M$ is the size-M identity matrix; $\mathbf{S} = \mathbf{F}_M$ amounts to frequency-domain sampling, where $\mathbf{F}_M$ is the M-point unitary discrete Fourier transform (FT) matrix. When $K < M$, reduced-rate sampling arises. We focus on non-adaptive measurements where $\mathbf{S}$ is preset.

The goal of CR sensing is to classify and estimate the spectrum of $r(t)$ given the sample set $\mathbf{x}_t$, where $K < M$ is possible. Spectrum classification refers to identifying the number of subbands N and their locations $\{[f_i, f_{i+1}]\}_{i=0}^{N-1}$, and classifying them into *black, gray or white* spaces. Spectrum estimation, on the other hand, can have different objectives: either to estimate the frequency response of $r(t)$ within the entire wideband, or confine the estimation to be within the identified (narrowband) white spaces only. This paper primarily concerns the coarse sensing task of spectrum classification.

3. MULTI-STEP COMPRESSED SENSING

Our first approach to reduced-complexity spectrum sensing takes the following four steps: *i*) compressed random sampling to generate measurements $\mathbf{x}_t$ from $r(t)$; *ii*) reconstruction of the frequency response $\mathbf{r}_f = \mathbf{F}_M \mathbf{r}_t$ from $\mathbf{x}_t$; *iii*) estimation of frequency band number N and locations $\{f_i\}_{i=1}^{N-1}$ based on $\hat{\mathbf{r}}_f$; and, *iv*) estimation of the average amplitude of $\mathbf{r}_f$ within each identified band for spectrum classification. It is worth emphasizing that Step *ii*) recovers the accurate fine-resolution signal spectrum $\mathbf{r}_f$ represented by M frequency samples at the Nyquist rate, while the available measurement set $\mathbf{x}_t$ is of a reduced size of $K(< M)$ elements.

3.1. Sub-Nyquist-rate Sampling

Let $\mathcal{F}$ denote the non-zero frequency-domain support of $r(t)$ in the noise-free case. In open-spectrum networks, it generally holds that $|\mathcal{F}| \ll B$ [4], indicating the sparseness nature of $r(t)$. Equivalently speaking, the $M \times 1$ frequency response vector $\mathbf{r}_f$ contains on average $K_b := \lceil |\mathcal{F}|M/B \rceil$ non-zero elements when noise free, and $K_b \ll M$. The key results in compressed sensing stated that the sparse vector $\mathbf{r}_f$ can be recovered asymptotically from K ($\leq M$) samples of $r(t)$, as long as $K \geq K_b$. These samples $\mathbf{x}_t$ can be generated from (1) via universal non-uniform sampling [5] or random sampling [6, 7], both of which can enable perfect recovery of $\mathbf{r}_f$ when free of noise. To distinct, we denote a reduced-rate sampling matrix as $\mathbf{S}_c$ of dimension $M \times K$, where $K_b \leq K \ll M$. A simple example of $\mathbf{S}_c$ is a selection matrix that randomly retains K columns of the size-M identity matrix, which means that $K - M$ time instants on the sampling grid are skipped.

3.2. Spectrum Reconstruction

With the K measurements $\mathbf{x}_t = \mathbf{S}_c^T \mathbf{r}_t$, we now estimate the frequency response of $r(t)$ in the form of $\mathbf{r}_f = \mathbf{F}_M \mathbf{r}$. For a given linear sampler $\mathbf{S}_c : \mathcal{C}^M \to \mathcal{C}^K$, we seek a nonlinear reconstruction function $R(\cdot) : \mathcal{C}^K \to \mathcal{C}^M$ that offers an approximate reconstruction of $\mathbf{r}_f \in \mathcal{C}^M$ from $\mathbf{x}_t \in \mathcal{C}^K$ based on the linear transformation equality $\mathbf{x}_t = (\mathbf{S}_c^T \mathbf{F}_M^{-1}) \mathbf{r}_f$; c.f. (1). This is a linear inverse problem with sparseness constraint, which is NP-hard. A conceptually intuitive approach to signal reconstruction is the Basis Pursuit (BP) technique [9], which transforms the sparseness constraint on $\mathbf{r}_f$ into a convex optimization problem solvable by linear programming:

$$\hat{\mathbf{r}}_f = \arg \min_{\mathbf{r}_f} ||\mathbf{r}_f||_1, \quad s.t. \quad (\mathbf{S}_c^T \mathbf{F}_M^{-1}) \mathbf{r}_f = \mathbf{x}_t. \tag{2}$$

Besides BP, a number of efficient reconstruction methods exist, including orthogonal matching pursuit (OMP) algorithm and tree-based OMP (TOMP) algorithm [8]. Since the measurements can be complex-valued, we find it convenient to use TOMP in our simulations, but for illustration, formulate our signal reconstruction problem based on BP, as in (2).

3.3. Band Location Estimation

Having estimated $\mathbf{r}_f$, we turn to the wavelet-based edge detector in [10] for detecting the number and frequency locations of spectrum spaces. The basic idea is to view the entire wideband under scrutiny as a train of consecutive frequency subbands, where the PSD is smooth within each subband, but exhibits a discontinuous change between adjacent subbands. These irregularities are in fact edges in PSD, which carry key information on the locations and intensities of spectrum holes. To further simplify and expedite the coarse sensing stage, we approximately treat the spectral amplitudes within each subband to be almost flat, at an unknown level α_n over the n-th band. These modeling approximations are invoked to reduce the overall wideband sensing complexity. If needed, the sensing quality can be refined after spectrum holes are identified.

Based on these modeling assumptions and with reference to Fig. 1, wideband sensing can be viewed as an edge detection problem in an image depicted by $\hat{\mathbf{r}}_f$ in frequency. Edges in this image correspond to the locations of frequency discontinuities $\{f_i\}_{i=1}^{N-1}$, which are to be identified. The wavelet approach is well motivated for edge detection [11]. Given $\hat{\mathbf{r}}_f$, we re-cast the edge detector in [10] in discrete form.

Let $\phi(f)$ be a wavelet smoothing function with a compact support. The dilation of $\phi(f)$ by a scale factor s is given by

$$\phi_s(f) = \frac{1}{s}\phi\left(\frac{f}{s}\right). \tag{3}$$

For dyadic scales, s takes values from powers of 2, i.e., $s = 2^j$, $j = 1, 2, \ldots, J$. Let $\Phi_s(\tau) := \mathcal{F}^{-1}\{\phi_s(f)\} = \Phi(s\tau)$ represent the inverse FT of the wavelet function. The continuous wavelet transform of $R(f)(\leftrightarrow \mathbf{r}_f)$ is given by [10]

$$\mathcal{W}_s R(f) = \mathcal{F}\{\mathcal{W}_s r(\tau)\} = \mathcal{F}\{r(\tau)\cdot\Phi(s\tau)\}. \tag{4}$$

Mapping $\mathcal{W}_s R(f)$, $r(\tau)$ and $\Phi(s\tau)$ to their length-M discrete counterparts $\mathbf{y}_s$, $\mathbf{r}_t$ and Φ_s respectively, (4) is equivalent to

$$\mathbf{y}_s = \mathbf{F}_M \text{diag}\{\Phi_s\}\mathbf{r}_t. \tag{5}$$

Replacing $\mathbf{r}_t$ in (5) by its estimate $\hat{\mathbf{r}}_t = \mathbf{F}_M^{-1}\hat{\mathbf{r}}_f$, we reach the estimated wavelet transform

$$\hat{\mathbf{y}}_s = \mathbf{F}_M \text{diag}\{\Phi_s\}\mathbf{F}_M^{-1}\hat{\mathbf{r}}_f. \tag{6}$$

The derivative wavelet of $\mathbf{r}_f$ at scale s is given by $\mathbf{z}_s$ with elements $\{z_s[n]\}_{n=1}^M$ in the form

$$s\frac{d}{df}\left(\mathcal{W}_s R(f)\right) \leftrightarrow \mathbf{z}_s:\ z_s[n] = y_s[n] - y_s[n-1]. \tag{7}$$

The boundaries $\{f_n\}_{n=1}^{N-1}$ can thus be acquired by picking the local maxima of the wavelet modulus $\mathbf{z}_s$, while the band number N is determined by the number of local peaks [10, 11].

3.4. Frequency Response Amplitude Estimation

The estimated boundaries $\{f_n\}_{n=1}^{N-1}$ correspond to $N-1$ selected indices $\{I_n : f_n = f_0 + I_n\Delta, \Delta = B/M\}$ in the frequency response vector $\mathbf{r}_f$. Elements of $\mathbf{r}_f$ between a pair of adjacent indices belong to the same frequency band. The average frequency response amplitude α_n of the n-th band, can thus be computed as

$$\hat{\alpha}_n \approx \frac{1}{I_n - I_{n-1} + 1}\sum_{i=I_{n-1}}^{I_n} |\hat{r}_f[i]|, \quad n = 1, \ldots, N. \tag{8}$$

This simple and coarse estimator in (8) allows us to categorize the detected frequency bands into *black, gray,* or *white* spaces [2], depending on whether $\{\hat{\alpha}_n\}$ are high, medium or low.

4. ONE-STEP COMPRESSED SENSING

To further reduce the implementation complexity of coarse spectrum sensing, we now ask: *can we directly detect and estimate the frequency band locations from the compressed measurements* $\mathbf{x}_t$ *in (1), without having to recover the detailed frequency response* $\mathbf{r}_f$? We address this question by deriving signal recovery formulation for wavelet-based edge detection.

Recall from Section 3.3 that the band locations can be recovered from the $(N-1)$ peaks of the derivative wavelet modulus $\mathbf{z}_s \in \mathcal{C}^M$. When $N \ll M$ (which is generally the case), $\mathbf{z}_s$ can be treated as a sparse vector, with only a few nontrivial elements located at frequency band boundaries; c.f., see Fig. 3 for graphical validation. As such, $\mathbf{z}_s$ can be recovered under the sparseness constraint, provided that we can find a linear transformation equality linking $\mathbf{z}_s$ to the compressed measurement vector $\mathbf{x}_t$.

To this end, we rewrite (7) in matrix-vector form as $\mathbf{z}_s = \Gamma\mathbf{y}_s$, where Γ is the differentiation matrix given by

$$\Gamma = \begin{bmatrix} 1 & 0 & \cdots & 0 \\ -1 & 1 & \ddots & 0 \\ 0 & \ddots & \ddots & \\ 0 & \cdots & -1 & 1 \end{bmatrix}_{M\times M}. \tag{9}$$

Putting (9) and (5) together, we obtain:

$$\mathbf{r}_t = \left(\mathbf{F}_M^{-1}\text{diag}\{\Phi_s\}\right)^{-1}\mathbf{y}_s = \underbrace{\left(\mathbf{F}_M^{-1}\text{diag}\{\Phi_s\}\right)^{-1}\cdot\Gamma^{-1}}_{:=\mathbf{G}}\cdot\mathbf{z}_s. \tag{10}$$

Noting that $\mathbf{x}_t = \mathbf{S}_c^T\mathbf{r}_t$, and that $\mathbf{z}_s$ is sparse, we reach the following BP-based optimization formulation:

$$\hat{\mathbf{z}}_s = \arg\min_{\mathbf{z}_s}||\mathbf{z}_s||_1, \quad s.t.\ \ \mathbf{x}_t = \left(\mathbf{S}_c^T\mathbf{G}\right)\mathbf{z}_s. \tag{11}$$

Subsequently, the band boundaries $\{f_n\}$ can be acquired from the locations of those non-zero elements in $\mathbf{z}_s$, obviating the involved step of frequency response estimation on $\mathbf{r}_f$.

5. SIMULATIONS

We consider a wide band of interest in the range of $f_0 + [50, 150]\Delta$ Hz, where Δ is the frequency resolution. Fig. 2 illustrates the spectral amplitude $|R(f)|$ observed by a CR. During the observed burst of transmissions in the network, there are a total of $N = 6$ bands, with frequency boundaries at $\{f_n\}_{n=1}^{6} = f_0 + [60, 68, 83, 119, 123, 150]\Delta$ Hz. Among these bands (marked in Fig. 2), B_1, B_3 and B_5 have relatively high signal amplitude at levels 16, 20, and 24, respectively, while B_2 has low amplitude at a level of 2. The rest two bands, B_4 and B_6 are not occupied and are thus white spectrum holes. The sampling lower bound is thus $K_b/M \approx 40\%$.

For compressed sensing, the compression ratio K/M is set to vary from 50% to 100% with reference to the Nyquist rate. The noise level is $n_w^2 = 8$ dB. The sampler $\mathbf{S} = \mathbf{S}_c$ used in (1) is uniformly random. Fig. 2 indicates that the signal recovery quality (via TOMP) improves as K/M increases.

In the wavelet-based edge detector, Gaussian wavelets are used at four dyadic scales $s = 2^j$, $j = 1, 2, 3, 4$. Fig. 3 depicts the multiscale wavelet products computed from (7) [10]. Edges in the $R(f)$ are clearly captured by the wavelet transform in all curves. As the scale factor s^j increases, the wavelet transform becomes smoother within each frequency band, retaining the lower-variation contour of the noisy PSD.

For frequency band location estimation, Fig. 4 depicts the normalized root mean-square estimation errors (RMSE) $B^{-1}\sqrt{\sum_{n=1}^{N-1} |f_n - \hat{f}_n|^2}$ with respect to both the compression ratio K/M and the inverse noise level n_w^{-2}. When either the number of samples is very small or the noise is very strong, there exhibits an estimation error floor. Nevertheless, the attained degree of estimation accuracy is beneficial to effecting CR agility at affordable sampling cost. Robustness to sample quantization errors is also illustrated.

6. REFERENCES

[1] "Facilitating Opportunities for Flexible, Efficient, and Reliable Spectrum Use Employing Cognitive Radio Technologies," FCC Report and Order, FCC-05-57A1, March 2005.

[2] S. Haykin, "Cognitive radio: brain-empowered wireless communications," *IEEE JSAC*, vol. 23(2), pp. 201-220, Feb. 2005.

[3] H. Urkowitz, "Energy detection of unknown deterministic signals," *Proc. of the IEEE*, vol. 55(4), pp. 523 - 531, April 1967.

[4] A. Sahai, D. Cabric, "Spectrum Sensing – Fundamental Limits and Practical Challenges," A tutorial presented at *IEEE DySpan Conference*, Baltimore, Nov. 2005.

[5] P. Feng, and Y. Bresler, "Spectrum-blind mimimum rate sampling and reconstruction of multiband signals," *Proc. IEEE Intl. Conf. on ASSP*, Atlanta, pp. 1688-1691, 1996.

[6] E. J. Candes, J. Romberg and T. Tao, "Robust Uncertainty Principles: Exact Signal Reconstruction from Highly Incomplete Frequency Information," *IEEE Trans. on Information Theory*, vol. 52, pp. 489-509, Feb. 2006.

[7] D. L. Donoho, "Compressed Sensing," *IEEE Trans. on Information Theory*, vol. 52, pp. 1289-1306, April 2006.

[8] C. La, and M. N. Do, "Signal reconstruction using sparse tree representation." *Proc. SPIE Conf. on Wavelet Apllications in Signal and Image Processing*, San Diego, Aug. 2005.

[9] S. S. Chen, D. L. Donoho, and M. A. Saunders, "Atomic decomposition by basis pursuit," *SIAM J. Sci. Comput.*, vol. 20, no. 1, pp. 33-61, 1999.

[10] Z. Tian, and G. B. Giannakis, "A Wavelet Approach to Wideband Spectrum Sensing for Cognitive Radios," *Proc. of Intl. Conf. on CROWNCOM*, Mykonos, Greece, June 2006.

[11] S. Mallat, W. Hwang, "Singularity detection with wavelets," *IEEE Trans. Info. Theory*, vol.38, pp. 617-643, 1992.

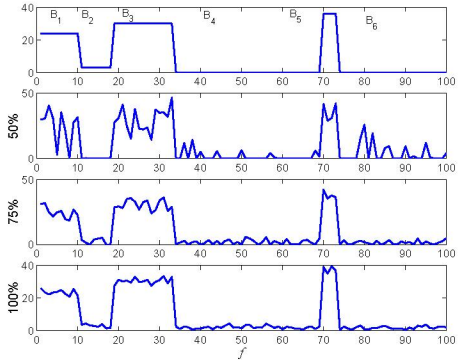

Fig. 2. signal frequency response: (top) noise-free $|X_f|$; (rest) recovered $|\hat{X}_f|$ at compressing ratios $K/M = 50\%, 75\%, 1$.

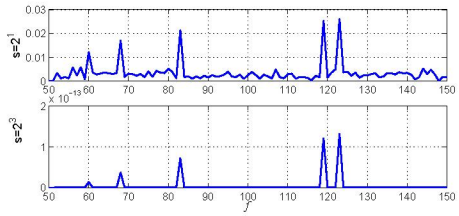

Fig. 3. wavelet modulus for edge detection at scales $s = 2^j$.

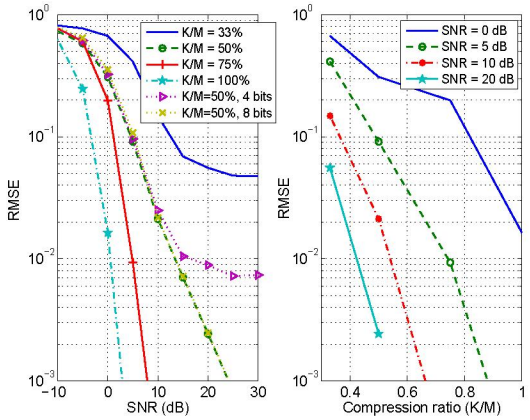

Fig. 4. frequency band location estimation errors RMSE. Strong compression of $K/M = 33\%$ is demonstrated. Impact of quantization (bits/sample) is shown for $K/M = 50\%$.